MAUSAM, **58**, 3 (July 2007), 351-360

551.577.3 (1-928.8)

Inter-annual variability of rainfalls in the Amazon basin and its vicinity

R. P. KANE

Instituto Nacional de Pesquisas Espaciais

C.P. 515, 12245-970 – São José dos Campos, SP, Brazil

(*Received 3 April 2006, Modified 22 August 2006*)

e mail : kane@dge.inpe.br

सार – अमेजन नदी बेसिन और इसके निकटवर्ती क्षेत्रों (15° उ.– 20° द., 30° – 80° प.) की वर्षा के 5°× 5° ग्रीडयुक्त आंकड़ों की श्रंखलाओं (12 माह की अवधि के गतिमान माध्यों) का विश्लेषण करने से यह पता चला है कि इस दौरान हुई वर्षा प्रति वर्ष और प्रति क्षेत्र दोनों में अत्याधिक रूप से परिवर्तनशील रही है। यहाँ तक कि निकटवर्ती क्षेत्रों के साथ सहसंबधं 0.50 से अधिक नहीं रहे है जबकि ये सहसंबंध ब्रजील के पूर्वी तट के निकटवर्ती क्षेत्रों में इससे बेहतर (0.70 तक) पाए गए हैं। इनसो के अक्षांकों समेत अमेज़न नदी बेसिन और इसके उत्तर में स्थित क्षेत्रों तथा उत्तरपूर्वी ब्राजील के साथ सामान्य संबंध रहे हैं। जबकि दक्षिण एटलांटिक एस. एस. टी. के साथ उत्तरपूर्वी ब्राजील और इसके पश्चिम के एकदम निकटवर्ती क्षेत्रों के सामान्य संबंध रहे हैं। अनय सभी संबंध (30 है. पा. पवन, उत्तरी एटलांटिक दोलन सूचकांक आदि सहित) अस्पष्ट थे।

ABSTRACT. An analysis of the rainfall series (12-month running means) of the 5° × 5° gridded data in the Amazon river basin and its vicinity (15° N – 20° S, 30° - 80° W) indicated that the rainfalls were highly variable both from year to year and from region to region. Correlations with even nearby regions hardly exceeded 0.50, though correlations were better (up to 0.70) in the regions near the eastern coast of Brazil. Moderate relationship with ENSO indices was obtained for the Amazon river basin and the regions to its north, and for NE Brazil, while moderate relationship with South Atlantic SST was obtained for NE Brazil and the region immediately to its west. All other relationships (with 30 hPa wind, North Atlantic Oscillation Index, etc.) were obscure.

Key words – ENSO, SST, OLR, Sub-tropical westerly jets, Inter-tropical convergence zone.

1. Introduction

The Amazon basin plays a very prominent role in the South American region. The precipitation may vary considerably from one small region to another in the same basin. In coastal Peru, heavy rainfall is considered as one of the criteria for identifying an El Niño event (Quinn *et al*., 1978, 1987; Quinn, 1992). Recently, Kane (2000) showed that the rainfall characteristics at Huancayo (central Peruvian Andes) were different from those of coastal Peru. Tarras-Wahlberg *et al*. (2003) showed that for rainfall patterns and river flows in southwestern Ecuador and northern Peru, El Niño events were important in regulating rainfall, but their significance diminished inland of the coastal plain. On the other hand, ENSO effects on rainfall in South America are reported to be mostly droughts in NE Brazil and excess rains in the southern parts, including Chile (Quinn and Neal, 1983; Aceituno, 1988; Ropelewski and Halpert, 1987, 1989; Rutland and Fuenzalida, 1991; Pisciottano *et al*., 1994; Diaz *et al*., 1998; Grimm *et al*., 1998; Robertson *et al*., 2001; see detailed references in Kane, 2002). For the Amazon basin, Marengo (1992) mentioned that whereas northern Amazonia showed strong El Niño signals, southern Amazonia seemed to be more independent of El Niño, and rainfall anomalies in northern Amazonia were associated with distinct circulation patterns in the tropical Atlantic. Also, ENSO effects may be different for different sizes of the basins. Marengo and Hastenrath (1993) presented case studies for the moderately wet year 1986 and the extremely dry El Niño year 1983 in northern Amazonia, where differences in locations of inter-tropical convergence zone (ITCZ), strength of subtropical westerly jets (STWJ), and vertical motions and convection over the Amazon basin were noticed. Zeng (1999) made an analysis of the Amazon basin hydrological cycle using data of rainfall and historical Amazon River discharge and reported a correlation with ENSO (El Niño/Southern Oscillation) of 0.8 for 1985-1993 and 0.56 for 1979-1996. Fu *et al.* (1999) examined the influence of atmosphere and land surface on the seasonal changes of convection in the tropical Amazon, while Fu *et al.* (2001) explored the influence of tropical SST on the seasonal distribution of precipitation in the equatorial Amazon. Marengo *et al.*

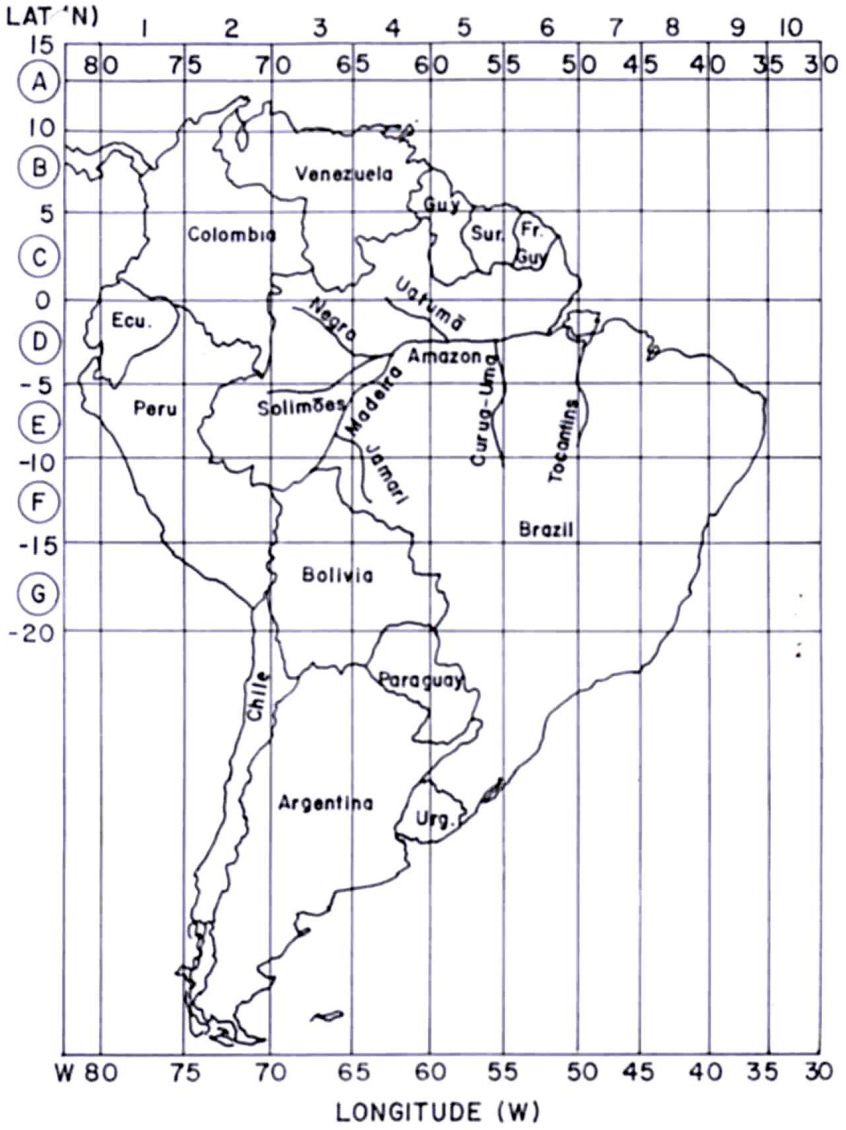

Fig. 1. Map of the Amazon basin and its vicinity, latitudes 15° N - 20° S, longitudes 30° - 80° W

(1993) reported that abundant rainy seasons in northern Amazonia were associated with cold SST in the tropical eastern Pacific and negative/positive anomalies in the tropical North/South Atlantic, accelerated Northeast trades and a southward displaced ITCZ. Liebmann *et al*. (1998) compared the rainfall, Outgoing Longwave Radiation (OLR) and divergence over the Amazon basin and found moderate correlation (~0.6 or less). The major seasonal transitions from dry to rainy regimes were captured well by OLR while the mean diurnal cycle was represented reasonably well by the 150 hPa divergence. Marengo *et al*. (2001) examined the onset and end of the rainy season in the Brazilian Amazon basin and found an apparent association between SST anomalies in the tropical Atlantic and Pacific and the onset and end dates in parts of the Amazon. Liebmann and Marengo (2001) found that areas of rainfall exhibiting strong relationship with SST were confined to the equatorial region of the Brazilian Amazon.

In the present communication, the rainfall characteristics are examined for the Amazon basin and its vicinity for a fine latitude-longitude grid of 5° × 5°, in the broad range of 15° N - 20° S, 80° W - 30° W, where the river Amazon and its tributaries are mainly in the range 0-10° S, 70 - 50° W (Fig. 1).

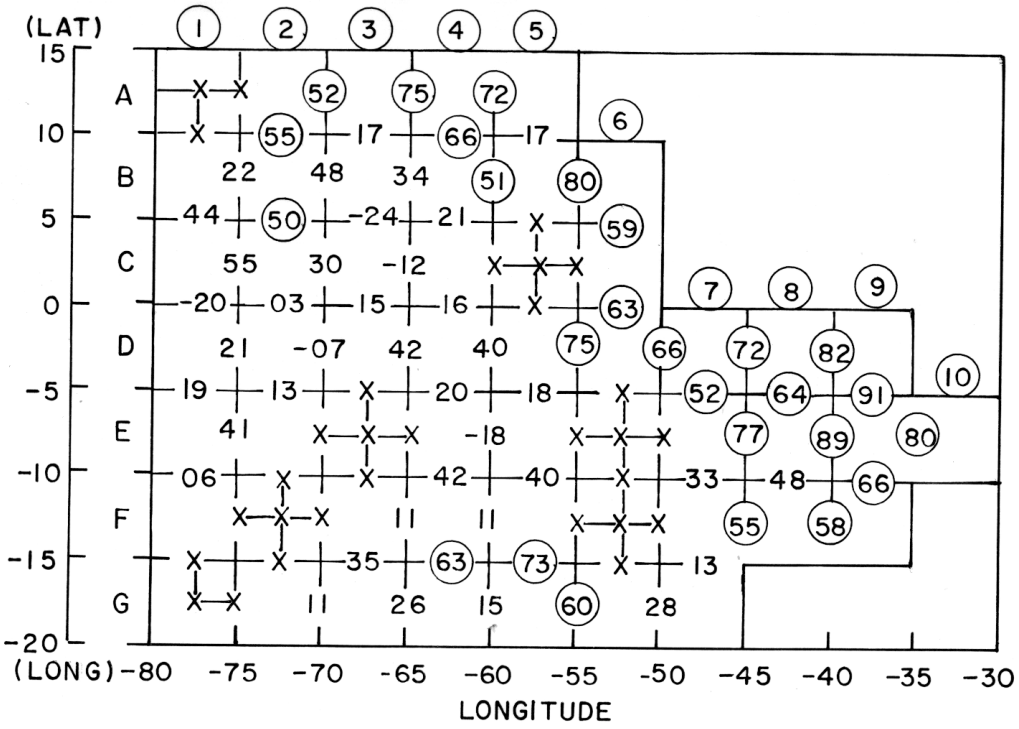

Fig. 2. Correlations between adjacent grids (B1 with B2, B2 with B3 etc., B1 with C1, C1 with D1, etc.). Correlations 0.50 or more are circled

2. Data

Data for gridded rainfall (Mitchell *et al*. 2002) were obtained from the website http://www.cru.uea.ac.uk/cru/data/hrg.htm. Data for seven climatic indices, namely, (1) 30 hPa low latitude zonal wind, El Niño/Southern Oscillation (ENSO) indices (2) Southern Oscillation Index represented by Tahiti (T) minus Darwin (D) atmospheric pressure difference T-D; and (3) Pacific Sea surface temperature SST for region Nino 1 + 2, 0 - 10° S, 90° - 80° W), (4) North Atlantic Oscillation (NAO) Index, (5) North Atlantic SST, (6) South Atlantic SST, (7) Tropical Atlantic SST, were obtained from the websites http://www.cpc.ncep.noaa.gov/data/indices/, http://www.cru.uea.ac.uk/ftpdata/nao.dat. For rainfall, the latitude and longitude belts were designated as :

A Lat.	15° N - 10° N	1 Long.	80° W - 75° W
B Lat.	10° N - 05° N	2 Long.	75° W - 70° W
C Lat.	05° N - 00°	3 Long.	70° W - 65° W
D Lat.	00° - 05° S	4 Long.	65° W - 60° W
E Lat.	05° S - 10° S	5 Long.	60° W - 55° W
F Lat.	10° S - 15° S	6 Long.	55° W - 50° W
G Lat.	15° S - 20° S	7 Long.	50° W - 45° W
		8 Long.	45° W - 40° W
		9 Long.	40° W - 35° W
		10 Long.	35° W - 30° W

Reliable continuous data for rainfall were available only for 1965-1990.

3. Climatology

The average rainfall seasons were not similar for all grids. Details of the climatology are not studied here. Instead, the average monthly values (climatology) are subtracted from the monthly values and thus, deseasoned monthly values are obtained. For further smoothing, 12-month running means are calculated.

4. Intercorrelations of rainfall series

To see whether the rainfall variations were similar in any regions, the yearly values are intercorrelated. Fig. 2 shows the correlation values (×100) for adjacent regions (A2 with A3, A3 with A4 etc.; A2 with B2, B2 with C2, etc.). As can be seen, many correlations are very low, even negative. Correlations of 0.50 or more are marked by circles. Most of these are near the coastal areas in the east part of the S. American continent. Thus, in the rest of the region, individual grids have intercorrelations less than 0.50, indicating only ~25% coherence, and large random components, *i.e*., highly localized characteristics due to various geographical reasons, including orographic effects. As such, global effects would be diluted.

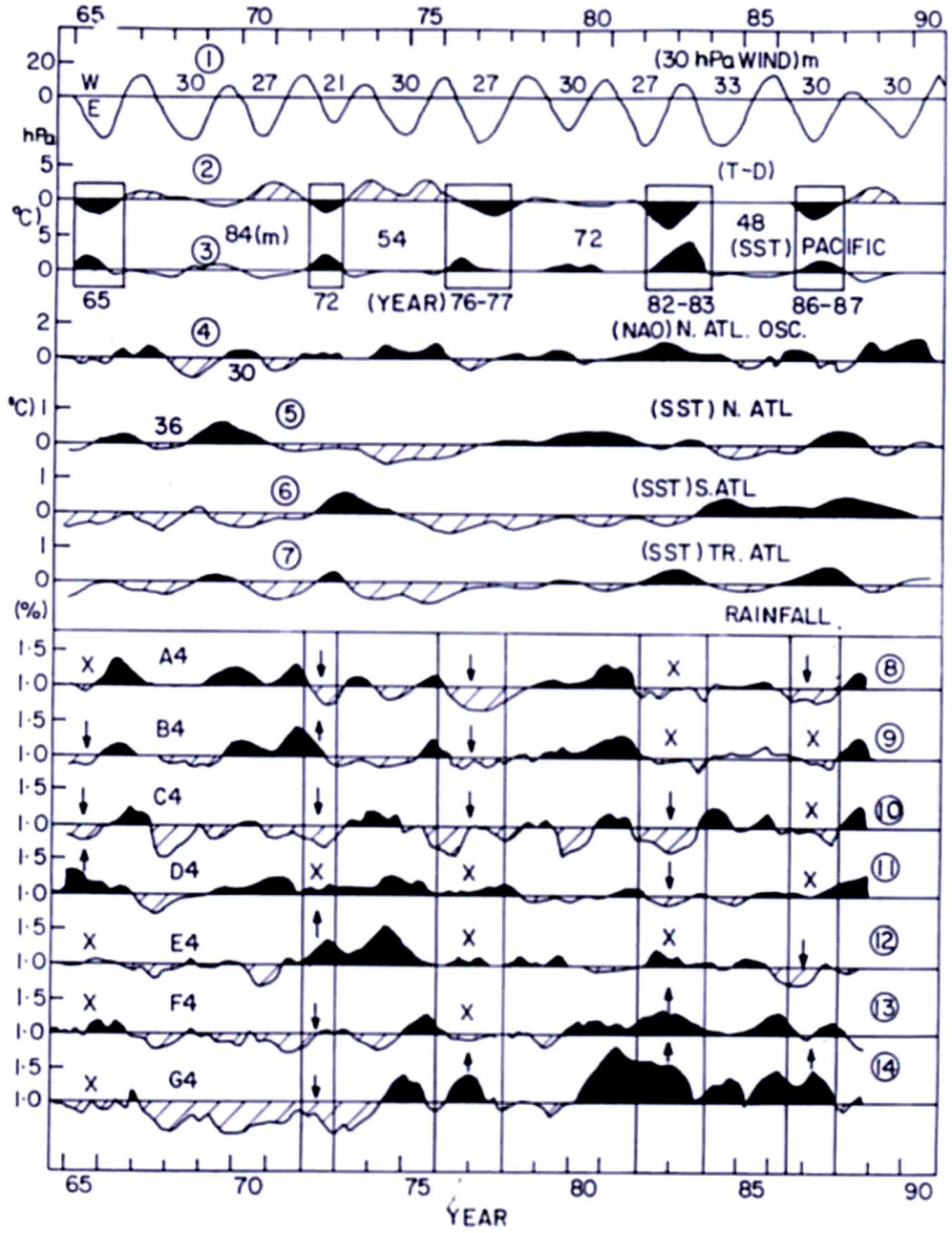

Fig. 3. Plots of the 12-month running means 3 months apart (4 values per year) for 1965-1990 for climatic indices (1) 30 hPa wind; (2) ENSO index T-D; (3) ENSO index SST Nino 1+2 in Pacific; (5, 6, 7), SST in North, South and Tropical Atlantic, and rainfall series (8-14) for latitudes A-G in the longitude belt 4 (60° - 65° W). Positive deviations are painted black and negative deviations are shown hatched (for T-D plot 2, negative deviations implying El Niños are painted black and positive are shown hatched). For 30 hPa wind (plot 1), maxima are indicated by dots and numbers indicate spacings in months between successive maxima. Arrows imply: pointing down - rainfall deficit; pointing up - rainfall excess; crosses - no effect

5. A sample plot

Fig. 3 (lower half) shows a sample plot of the 12-month running means of rainfall, centered 3 months apart (4 values per year) for the longitude belt 4 (60° - 65° W) for latitudes A-G (15° N - 20° S). Positive deviations (excess rains) are shown black, and negative deviations (deficit rains) are shown hatched. The upper half of Fig. 3

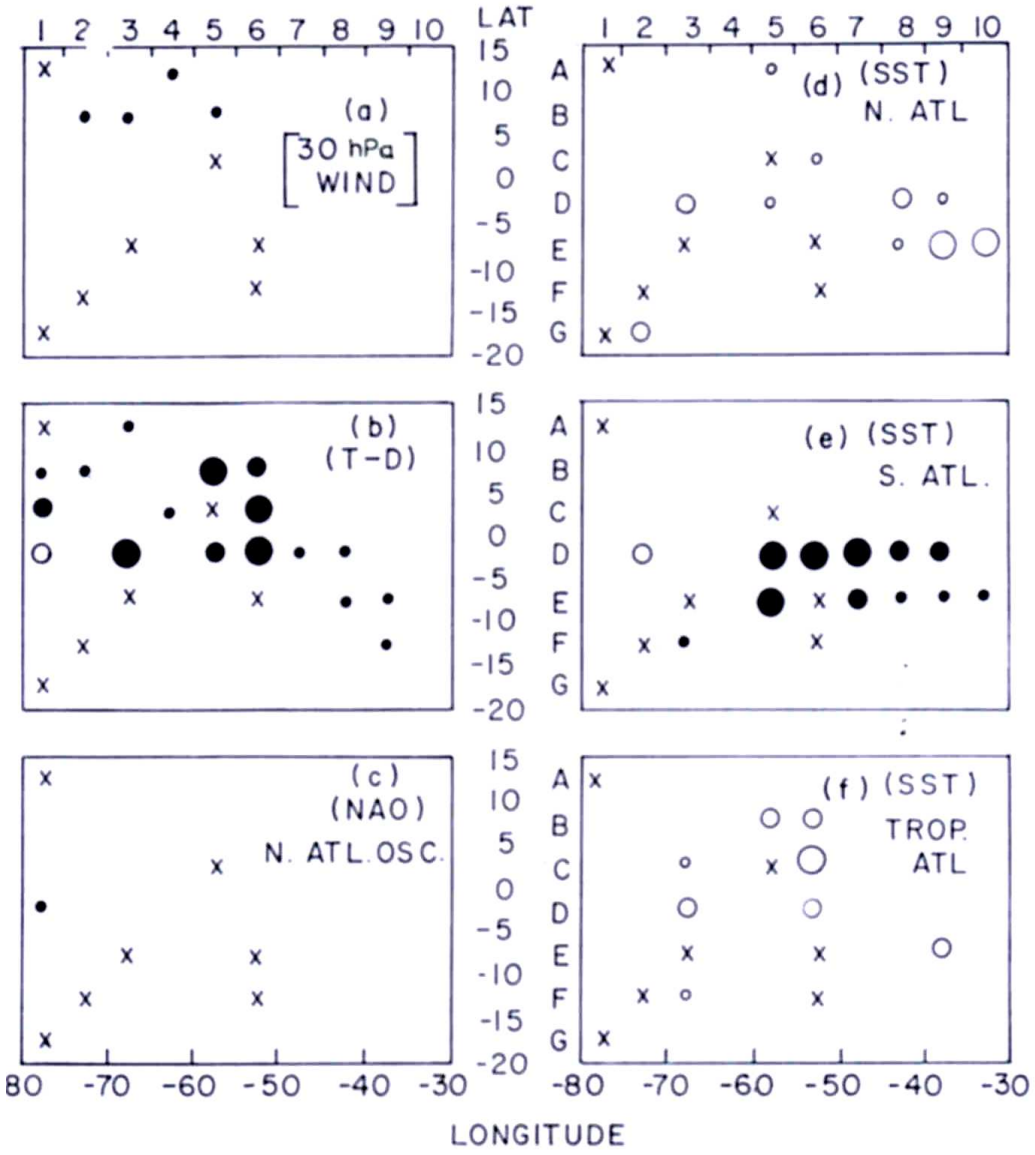

Figs. 4(a-f). Correlations of rainfalls in various grids with (a) 30 hPa wind, (b) ENSO index T-D, (c) North Atlantic Oscillation Index NAO, (d, e, f) North Atlantic, South Atlantic and Tropical Atlantic SST. Crosses show missing data. Small, medium and big circles indicate correlations in the ranges 0.40-0.50, 0.50-0.60, more than 0.60. Full shaded circles indicate positive correlations and open circles indicate negative correlations

shows plots for seven climatic indices considered for relationship with rainfall. The top plot is for 30 hPa low latitude zonal winds and shows mainly a Quasi-biennial oscillation (QBO) with peak spacings in the range 21-33 months (1.8-2.8 years). The next plot is for the Southern Oscillation Index T-D. The negative values are shown black and indicate the presence of El Niños. The third plot is for Pacific SST for the Nino 1+2 region (0 - 10° S, 90° - 80° W), and the positive values are shown black, again indicating El Niños. There were five major El Niño events, in 1965, 1972, 1976-1977, 1982-1983, 1986-1987, with spacings of 84, ~54, 72, and 48 months (4-7 years). Their relationship with rainfalls is indicated by arrows on the rainfall plots, a downward pointing arrow implying deficit rainfall, an upward pointing arrow implying excess rainfall, and a cross implying no effect. As can be seen, some latitudes show deficit rains, others show excess rains, and some show no relationship at all. Also, not all

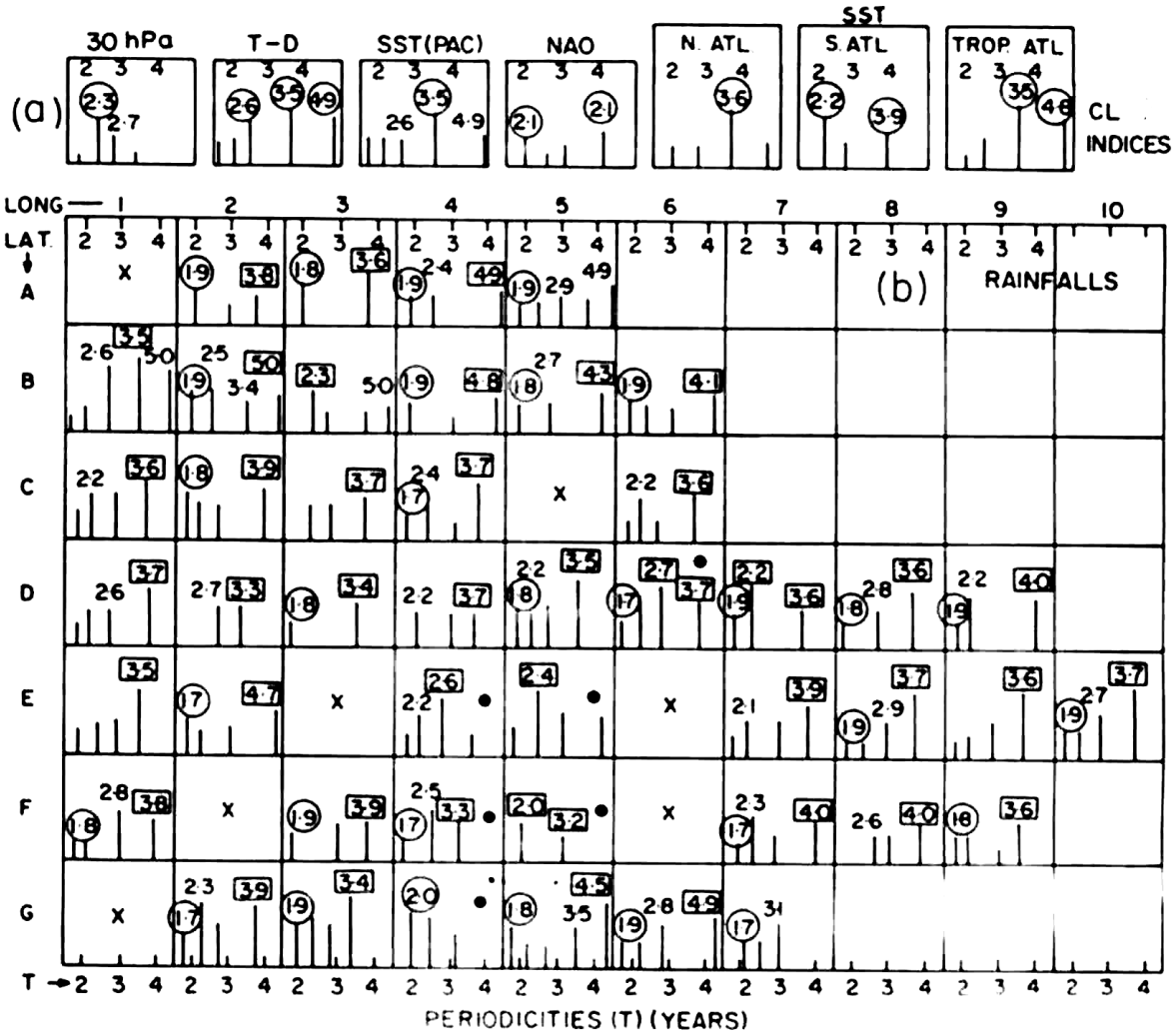

Figs. 5(a&b). Spectra amplitudes *versus* periodicities T detected by MEM for 1965-1990, for (a) climatic indices and (b) rainfalls in latitudes A-G, longitudes 1-10. Numbers are periodicities T in years

El Niños are equally effective. In addition, several deficit rainfalls seem to have occurred when there were no El Niños. Thus, rainfall relationship with El Niño/Southern Oscillation (ENSO) phenomenon is highly variable from region to region and is uncertain. Plots similar to Fig. 3 for longitude belt 4, were made for other longitude belts (1-3, 5-10). All showed similar uncertainties and variability of ENSO effects. Some of the variations in rainfall may not be related to ENSO but may be related to other parameters (NAO, Atlantic SST, etc.).

6. Rainfall correlations with climatic indices

The various rainfall series were correlated with seven climatic indices. The ENSO indices T-D and Pacific SST showed almost exactly opposite correlations (positive with T-D, negative with SST, or *vice versa*). Hence, only T-D is considered. Figs. 4(a-f) shows the correlations for each grid of rainfall (latitudes A-G, longitudes 1-10) with six climatic indices (a) 30 hPa wind, (b) T-D, (c) NAO, (d) North Atlantic SST, (e) South Atlantic SST, (f) Tropical Atlantic SST. The crosses indicate missing rainfall data (grids A1, C5, E3, E6, F2, F6, G1). Positive correlations are shown with full circles of different sizes: small, correlation 0.40-0.50; moderate, 0.50-0.60; large, 0.60 and more (classification arbitrary). Negative correlations are shown with open circles, in similar size ranges. The following may be noted:

(*i*) In (a), there are only three small correlations, one moderate correlation, and no large correlations. Thus, relationship with 30 hPa wind is almost non-existent.

(*ii*) In (b), there are large correlations with T-D only in a restricted region (B5, B6, C6, D3, D5, D6) which consists of the Amazon river and the regions to its north. Moderate correlations are seen in D, E, F; 7, 8, 9, 10, which is the region NE Brazil.

(*iii*) In (c), the NAO has virtually no moderate or large correlations in any region.

(*iv*) In (d), the North Atlantic SST has large negative correlations mostly for NE Brazil.

(*v*) In (e), the South Atlantic SST has large positive correlations with NE Brazil and the region immediately to its west.

(*vi*) In (f), the tropical Atlantic seems to have a few high negative correlations in the region north of Amazon river (Guyana, Surinam).

Overall, the T-D and South Atlantic SST seem to have a reasonably good relationship with rainfall in the Amazon basin and the NE Brazil. All other relationships are poor.

7. Spectral analysis

To obtain quantitative estimates of the spectral characteristics of the inter-annual variability, the series in Fig. 3 (about 100 seasonal values) were subjected to spectral analysis by MEM (Maximum Entropy Method, Burg, 1967; Ulrych and Bishop, 1975), which locates peaks much more accurately than the conventional BT (Blackman and Tukey, 1958) method. However, the amplitude (Power) estimates in MEM are not very reliable (Kane, 1977, 1979; Kane and Trivedi, 1982). Hence, MEM was used only for detecting all the possible peaks T_k (k = 1 to n), using LPEF (Length of the Prediction Error Filter) as 50% of the data length. These T_k were then used in the expression:

$$f(t) = A_o + \sum_{k=1}^{n} [a_k \sin(2\pi t/T_k) + b_k \cos(2\pi t/T_k)] + E$$

$$= A_o + \sum_{k=1}^{n} r_k \sin(2\pi t/T_k + \phi_k) + E$$

where $f(t)$ is the observed series and E the error factor. A Multiple Regression Analysis (MRA, Bevington. 1969) was then carried out to estimate A_o (a_k. b_k), and their standard errors (by a least-square fit). From these, amplitudes r_k and their standard error σ_k (common for all r_k in this methodology, which assumes white noise) were calculated. Any r_k exceeding 2σ is significant at a 95% (a priori) confidence level.

Figs. 5(a&b) shows the spectra (amplitudes, *versus* periodicities T detected by MEM) for the seven climatic indices and for the various rainfall series. Only peaks significant at a 2σ or better level are shown. The following may be noted:

(*i*) The first row refers to the seven climatic indices.

(*ii*) The 30 hPa wind has only QBOs, one prominent periodicity at 2.3 years (28 months) and a subsidiary periodicity at 2.7 years (32 months), resulting in the wide range of spacings (21-33 months) in the 30 hPa plot in Fig. 3.

(*iii*) The ENSO indices T-D and Pacific SST are characterized by two prominent periodicities at 3.5 (QTO, quasi-triennial oscillation) and 4.9 years and a subsidiary periodicity at 2.6 years (QBO).

(*iv*) NAO has one major periodicity at 4.1 years and a minor periodicity at 2.1 years (QBO, different from the 2.3 years of 30 hPa wind or 2.6 years of ENSO indices).

(*v*) The North Atlantic and Tropical Atlantic SST have a major periodicity at ~3.5 years (QTO) and a minor periodicity at ~4.8 years, almost the same as 3.5 years (QTO) and 4.9 years of the ENSO indices. Hence, the effects of North and Tropical Atlantic SST cannot be distinguished from those of ENSO indices.

(*vi*) The South Atlantic SST has a major periodicity at 2.2 years (QBO, same as 2.3 of 30 hPa wind) and a minor periodicity at 3.9 years (different from the 3.5 years of ENSO indices, but almost similar to 4.1 years of NAO.

The other rows show the spectra for the various rainfall series (latitudes A-G, longitudes 1-10). Following may be noted:

(*i*) The periodicities are not all similar in all the rainfall grids, as expected. Characteristics are partly similar and partly different.

(*ii*) Most of the rainfall series have a small but statistically significant (above 2σ) peak near 1.7-1.9 years (20-23 months). No climatic index has such a peak.

(*iii*) Many rainfall series have prominent QTOs near 3.5 years and subsidiary peaks in the QBO region, thus indicating ENSO influence. However, a few regions (marked by a full dot) namely, D6; E4, E5; F4, F5; G4, have a QBO (2.0-2.7 years) more prominent than the QTOs. These regions are to the south of the Amazon river

up to the Bolivian border (Fig. 1) and their rainfalls may be related to 30 hPa winds (QBOs at 2.3 years and 2.7 years) or South Atlantic SST (major QBO at 2.2 years).

(*iv*) Many regions show periodicities at 3.5-3.6 years (11 regions: A3; B1; C1, C6; D5, D7, D8; E1, E9; F9; G5) and 4.7-5.0 years (8 regions: A4, A5; B1, B2, B3, B4; E2; G6) and these probably indicate ENSO effects (or North and Tropical Atlantic SST effects) near 3.5 and 4.9 years.

(*v*) Some regions show periodicities at 3.1-3.4 years (7 regions : B2; D2, D3; F4, F5; G3, G7), which are not similar to the ENSO indices or to any other climatic index.

(*vi*) Some regions show 3.7 years (7 regions: C3, C4; D1, D4, D6; E8, E10), 3.8 years (A2; F1), 3.9 years (C2; E7; F3; G2), 4.0 years (D9; F7, F8), 4.1 years (B6), 4.3 years (B5), 4.5 years (G5), which are significantly larger than the ~3.5 years and smaller than the 4.7-5.0 year range of the ENSO indices, and cannot be identified unambiguously as ENSO effects but some could be related to the 4.1 years of NAO and the 3.9 years of South Atlantic SST.

Overall, no effects are overwhelming (earlier, correlations hardly exceeding 0.7, so 50% or more variance remained unexplained), but moderate ENSO effects and/or South Atlantic SST effects exist for some regions. This agrees with the correlation indications of Fig. 4.

8. Conclusions and discussion

An analysis of the rainfall series (12-month running means) of the 5° × 5° gridded data in the Amazon river basin and its vicinity (15° N - 20° S, 30° - 80° W) indicated the following:

(*i*) The rainfalls were highly variable both from year to year and from region to region. Correlations with even nearby regions hardly exceeded 0.50, indicating only ~25% coherence (75% random component). Correlations were better (up to 0.70, indicating 50% coherence) in the regions near the eastern coast of Brazil.

(*ii*) Moderate relationship with ENSO indices was obtained for the Amazon river basin and the regions to its north, and for NE Brazil.

(*iii*) Moderate relationship with South Atlantic SST was obtained for NE Brazil and the region immediately to its west.

(*iv*) All other relationships (with 30 hPa wind, North Atlantic Oscillation Index, etc.) were obscure.

ENSO effects in different parts of the globe have been reported since long (Ropelewski and Halpert, 1987, 1989) but these are never one-to-one. Also, these are often distorted by other effects. For example, in southern part of South America (including southern Brazil), El Niños are very well related to excess rains, but in NE Brazil, low latitude Atlantic temperature increases combined with favorable winds towards the Brazilian coast can bring in moisture which may neutralize the drought-like conditions caused by El Niños. In other parts of the world too, other factors complicate the ENSO relationship. In India, interannual variability of All India summer monsoon rainfall and its relationship with ENSO as well as with other factors (snow mass covers etc.) has been illustrated by many workers (Kripalani *et al*., 1996, 2003; Krishna Kumar *et al*., 1999; Krishnamurthy and Goswami, 2000; Rajeevan and McPhaden, 2004), and prediction schemes are used with eight or more parameters where only one is ENSO (Thapliyal and Rajeevan, 2003). In the Amazon basin, one would have expected that the vicinity to the Peru-Ecuador coast (birth place of El Niño) would result in strong ENSO effects. This does not seem to happen, probably because of other interfering effects like those related to tropical Atlantic, or local circulation patterns related to orographic effects, etc.

The spectral peaks in the Amazon rainfall series in the range 1.7-1.9 years (20-23 months) are intriguing. Indian rainfall series do not show significant peaks in this range (Kane, 1999), but some solar, interplanetary and geomagnetic parameters do show peaks in this range (Kane, 2005). The possible connection with rainfall series is not obvious and needs further exploration.

Acknowledgements

This work was partially supported by FNDCT, Brazil under contract FINEP-537/CT.

References

Aceituno, P., 1988, "On the functioning of the Southern Oscillation in the South American sector, Part I: Surface climate", *Mon. Wea. Rev.*, **116**, 505-524.

Bevington, P. R., 1969, "Data reduction and error analysis for the physical sciences", McGraw-Hill, New York, 164-176.

Blackman, R. B. and Tukey, J. W., 1958, "The measurement of power spectra", Dover, New York, p190.

Burg, J. P., 1967, "Maximum entropy spectral analysis", paper presented in October at the 37th Meeting, Society of Exploration, Oklahoma City.

Diaz, A. F., Studzinski, C. D. and Mechoso, C. R., 1998, "Relationships between precipitation anomalies in Uryguay and southern Brazil and sea surface temperature in the Pacific and Atlantic oceans", *J. Climate*., **11**, 251-271.

Fu, R., Zhu, B. and Dickinson, R. E., 1999, "How do atmosphere and land surface influence seasonal changes of convection in the tropical Amazon?", *J. Climate*, **12**, 1306-1321.

Fu, R., Dickinson, R. E., Chen, M. and Wang, H., 2001, "How do tropical sea surface temperatures influence the seasonal distribution of precipitation in the equatorial Amazon?", *J. Climate*, **14,** 4003-4026.

Grimm, A. M., Ferraz, S. E. T. and Gomes, J., 1998, "Precipitation anomalies in southern Brazil associated with El Niño and La Niña events", *J. Climate*, **11**, 2863-2880.

Kane, R. P., 1977, "Power spectrum analysis of solar and geophysical parameters", *J. Geomag. Geoelect*., **29**, 471-495.

Kane, R. P., 1979, "Maximum entropy spectral analysis of some artificial samples", *J. Geophys. Res.*, **84**, 965-966.

Kane, R. P., 1999, "Periodicities and ENSO relationships of the seasonal precipitation over six major sub-divisions of India", *Mausam*, **50**, 1, 43-54.

Kane, R. P., 2000, "El Niño/La Niña relationship with rainfall at Huancayo", in the Peruvian Andes, *Int. J. Climatol*., **20**, 63-72.

Kane, R. P., 2002, "Precipitation anomalies in southern South America associated with a finer classification of El Niño and La Niña events", *Int. J. Climatol*., **22**, 357-373.

Kane, R. P., 2005, "Differences in the quasi-biennial and quasi-triennial oscillation characteristics of the solar, interplanetary, and terrestrial parameters", *J. Geophys. Res*., **110**, A01108, doi:10.1029/2004JA010606.

Kane, R. P. and Trivedi, N. B., 1982, "Comparison of maximum entropy spectral analysis (MESA) and least-square linear prediction (LSLP) methods for some artificial samples", *Geophysics*, **47**, 1731-1736.

Kripalani, R. H., Singh, S. V., Vernekar A. D. and Thapliyal, V., 1996, "Empirical study on Nimbus-7 snow mass and Indian monsoon rainfall", *Int. J. Climatology*, **16**, 23-34.

Kripalani, R. H., Kulkarni, A., Sabade, S. S. and Khandekar, M. L., 2003, "Indian monsoon variability in a global warming scenario", *Nat. Hazards*, **29**, 189-206.

Krishna Kumar, K., Rajgopalan, B. and Cane, M. A., 1999, "On the weakening relationship between the Indian monsoon and ENSO", *Science*, **284**, 2156-2159.

Krishnamurthy, V. and Goswami, B. N., 2000, "Indian monsoon-ENSO relationship on interdecadal time scale", *J. Climate*, **13**, 579-595.

Liebmann, B. and Marengo, J. A., 2001, "Interannual variability of the rainy season and rainfall in the Brazilian Amazon Basin", *J. Climate*, **14**, 4308-4318.

Liebmann, B., Marengo, J. A., Glick, J. D., Kousky, V. E., Wainer, I. C. and Massambani, O., 1998, "A comparison of rainfall, outgoing long wave radiation, and divergence over the Amazon Basin", *J. Climate*, **11**, 2898-2909.

Marengo, J., 1992, "Interannual variability of surface climate in the Amazon basin", *Int. J. Climatol*., **12**, 853-863.

Marengo, J. A. and Hasrenrath, S., 1993, "Case studies of extreme climatic events in the Amazon basin", *J. Climate*, **6**, 617-627.

Marengo, J., A., Druyan, I. and Hastenrath, S., 1993, "Observational and modeling studies of Amazonia interannual climate variability", *Climatic Change*, **23**, 267-286.

Marengo, J. A., Liebmann, B., Kousky, V. E., Filizola, N. P. and Wainer, I. C., 2001, "Onset and end of the rainy season in the Brazilian Amazon Basin", *J. Climate*, **14**, 833-852.

Mitchell, T. D., Hulme, M. and New, M., 2002, "Climate data for political areas", *Area*, **34**, 109-112.

Pisciottano, G., Diaz, A., Cazes, G. and Mechoso, C. R., 1994, "El Niño-Southern Oscillation impact on rainfall", *J. Climate*, **7**, 1286-1302.

Quinn, W. H., 1992, "El Niño Historical and Paleoclimatic Aspects of the Southern Oscillation [Diaz. Henry and Marhgraf, V. (eds)]. Cambridge Press.

Quinn, W. H. and Neal, V. T., 1983, "Long-term variations in the southern oscillation. El Niño and the Chilean subtropical rainfall", Fishery Bulletin (USA), **81**, 363-374.

Quinn, W. H., Zoff, D. G., Short, K. S. and Kuo Yang, R. T. W., 1978, "Historical trends and statistics of the Southern Oscillation. El Niño and Indonesian droughts", *Fish. Bull*., **76**, 663-678.

Quinn, W. H., Neal, V. T. and Antunes de Mayolo, S. E., 1987, "El Nino occurrences over the past four and a half centuries", *J. Geophys. Res.*, **92**, 14449-14461.

Rajeevan, M. and McPhaden, M. J., 2004, "Tropical Pacific upper ocean heat content variations and Indian summer monsoon rainfall", *Geophys. Res. Lett.*, **31**, L18203, doi:10.1029/2004GL020631.

Robertson, A. W. and Mechoso, C. R. and Garcia, O. N., 2001, "Interannual prediction of the Paraná river", *Geophys. Res. Lett.*, **28**, 4235-4238.

Ropelewski, C. F. and Halpert. M. S., 1987, "Global and regional scale precipitation patterns associated with El Niño/Southern Oscillation", *Mon. Wea. Rev.*, **115**, 1606-1626.

Ropelewski, C. F. and Halpert. M. S., 1989, "Precipitation patterns associated with the high index phase of the southern oscillation", *J. Climate*, **2**, 268-289.

Rutland, J. and Fuenzalida, H., 1991, "Synoptic aspects of the central Chile rainfall variability associated with the Southern Oscillation", *Int. J. Climatol*., **11**, 63-76.

Tarras-Wahlberg, N. H., Caudwell, S. W. B. and Lane, S. N., 2003, "El Niño events, rainfall patterns and floods in the Puyango river basin, southern Ecuador", *Geografiska Annaler. Series A.* Physical Geography.

Thapliyal, V. and Rajeevan, M., 2003, "Updated operational models for long-range forecasts of Indian summer monsoon rainfall", *Mausam*, **54**, 495-504.

Ulrych, T. J. and Bishop, T. N., 1975, "Maximum entropy spectral analysis and autoregressive decomposition", *Rev. Geophys.*, **13**, 183-200.

Zeng, N., 1999, "Seasonal cycle and interannual variability in the Amazon hydrological cycle", *J. Geophys. Res.*, **104**, 9097-9106.